

Maximal Relevance and Optimal Learning Machines

O Duranthon¹, M Marsili², and R Xie³

¹Department of Physics, École Normale Supérieure, 24 rue Lhomond, 75005 Paris, France
²The Abdus Salam International Centre for Theoretical Physics, Strada Costiera 11, 34151 Trieste, Italy
³College of Physical Science and Technology, Central China Normal University (CCNU), Wuhan, China

Abstract

We show that the mutual information between the representation of a learning machine and the hidden features that it extracts from data is bounded from below by the relevance, which is the entropy of the model’s energy distribution. Models with maximal relevance – that we call Optimal Learning Machines (OLM) – are hence expected to extract maximally informative representations. We explore this principle in a range of models. For fully connected Ising models and we show that *i*) OLM are characterised by inhomogeneous distributions of couplings, and that *ii*) their learning performance is affected by sub-extensive features that are elusive to a thermodynamic treatment. On specific learning tasks, we find that likelihood maximisation is achieved by models with maximal relevance. Training of Restricted Boltzmann Machines on the MNIST benchmark shows that learning is associated with a broadening of the spectrum of energy levels and that the internal representation of the hidden layer approaches the maximal relevance that can be achieved in a finite dataset. Finally, we discuss a Gaussian learning machine that clarifies that learning hidden features is conceptually different from parameter estimation.

1 Introduction

Statistical mechanics models have been used in statistical learning since the pioneering works on associative memory [1] and on Boltzmann Learning Machines [2]. Many attempts to make sense of the spectacular performance of learning machines, such as deep neural networks, have focused on understanding their statistical mechanics properties, as compared e.g. to spin glasses [3]. It is widely believed that learning machines are characterised by some typical properties, such as the compositional phase discussed by [4] and its spectral properties [5], wide flat free energy minima [6] or criticality [7]. Yet, these properties only emerge after the interaction parameters have been learned from highly structured datasets [8, 9, 10]. In addition, the properties of learning machines also depend on what measure of error or likelihood is used in supervised or unsupervised learning, respectively. Hence, it hard to discuss the typical properties of learned models without reference to the particular dataset on which the model is trained, on the objective function assumed, on the algorithms or on the architecture used. This is why many attempts to understanding learning focus on the ingredients which makes it possible [11].

This is somewhat reminiscent of the state of affairs of heat engines two centuries ago, that had been powering the industrial revolution. A full theoretical understanding [12] of heat engines didn't come from the analysis of their ingredients, but from the analysis of ideal systems and the realisation that the key observables (work and heat) were related to state variables (energy and entropy), that ultimately impose fundamental limits to their efficiency.

This paper takes a similar perspective and expands on the approach proposed in [13]. This advocates that learning is about extracting relevant representations from data, rather than minimising errors or maximising likelihood. Relevance is quantitatively defined as follows: A learning machine maps the data \mathbf{x} , generated from an unknown generative model $p(\mathbf{x})$, to an internal representation \mathbf{s} , where \mathbf{s} are the state of the hidden layer(s) of the learning machine. Learning induces a distribution $p(\mathbf{s})$ on the hidden states and we define the energy $E_{\mathbf{s}} = -\log p(\mathbf{s})$ as the coding cost associated to a microscopic state \mathbf{s} . Hence the average energy

$$\langle E \rangle = - \sum_{\mathbf{s}} p(\mathbf{s}) \log p(\mathbf{s}) \equiv H[\mathbf{s}] \quad (1)$$

is a measure of the resolution of the representation. The entropy of the energy distribution

$$H[E] = - \sum_E p(E) \log p(E), \quad p(E) = \sum_{\mathbf{s}} p(\mathbf{s}) \delta(E - E_{\mathbf{s}}) \quad (2)$$

instead provides a quantitative measure of the information that the model contains on the generating process of the data, and is henceforth called *relevance*. We define Optimal Learning Machines (OLM) as statistical mechanics models that maximise the relevance at a given resolution $H[\mathbf{s}]$. In other word, the architecture of these models are such that the distribution of their energy levels is as broad as possible. This allows one to describe the properties of OLM without reference to the data with which they have been trained. This apparently paradoxical fact is rooted on the assumption that the data with which the learning machine is trained contains a rich structure and that the goal of learning is precisely to decompose this structure into a set of hidden features. This argument, which is developed in the next section, shows that the relevance $H[E]$ is a lower bound to the amount of information that the representation contain on the hidden features. Hence *models with maximal relevance, at a fixed resolution, are those that are mostly informative on the features hidden in the data*. As a corollary, OLM are machines that extract the most compressed representations from data, with an information content on the features which is at least of $H[E]$ bits.

This requirement implies an exponential distribution of energy levels, which is equivalent to statistical criticality [13]. The fact that this is a widely observed statistical regularity in efficient representations [7, 14, 15], corroborates the use of the principle of maximal relevance as a tool to understand learning machines.

The aim of this paper is to explore the principle of maximal relevance in the context of specific classes of models, in order to understand how closely real learning machines approximate the ideal limit of OLM. We shall first focus on the class of $J_{i,j} = \pm J$ fully connected Ising models, where the spectrum of energy levels is discrete. This sheds light on the properties of OLM and on their architectures. In particular, we discuss the statistical mechanics properties of OLM within this class, in order to contrast the properties of Ising OLM with those of well known models, such as the mean field Ising ferromagnet and the $J_{i,j} = \pm J$ spin glass. Our main findings are that *i*) properties that make models good learning machines may be related to sub-leading terms in a statistical mechanics analysis and may not be accessible to standard approaches, *ii*) OLM feature

heterogeneous architectures and *iii)* their properties are not necessarily related to the existence of a critical point separating two different phases.

Then we move to learning machines with a continuum spectrum of energy levels. This requires to redefine the relevance with respect to a discretisation of energy levels. We first focus on Restricted Boltzmann Machines, and we show that during learning the distribution of energy levels indeed broadens. For small systems, it is possible to follow the evolution of the spectrum of energy levels and we find that the internal representation undergoes cycles of relevance maximisation and compression. For larger systems, we show how to probe the statistical properties of the internal representation on the basis of a sample of draws from $p(\mathbf{s})$ using the Montecarlo Markov chain (MCMC) method. The natural discretisation is dictated by the number of samples on which the machine is trained. We show that, at this level of detail, RBM indeed converge to states of maximal relevance. Finally, we contrast our results with the analysis of a Gaussian learning machine, that aims at reproducing the first two moments of a dataset. This is instructive because we find that, in this case, the relevance $H[E]$ is independent of the data and learning only involves adjusting the resolution $H[\mathbf{s}]$ of the internal representation. This apparently paradoxical result is a consequence of the fact that, in a Gaussian world, features (means and covariances) are known *a priori*. There are no hidden features to learn. Learning concerns only the estimation of the parameters of a model (a multivariate Gaussian) with predefined features.

The next section discusses the principle of maximal relevance in the general context of feature extraction in learning. The following one, introduces the Ising learning machine. It first discusses OLM in this class for small systems through exact enumeration and then few specific architectures for large systems. We illustrate our result on two small test cases, where we find that likelihood maximisation in structured datasets indeed converges to OLM. Section 4 discusses models with a continuum spectrum of energy levels, i.e. RBMs and the Gaussian learning machine.

We summarise and comment our results in the concluding section.

2 Relevance lower bounds the mutual information between data and hidden features

Let us assume that data points $\mathbf{x} = (x_1, \dots, x_d)$ are generated as draws from an unknown distribution $p(\mathbf{x})$ that is characterised by a rich structure of dependence between the components x_a . For example, the benchmark MNIST dataset [16] of hand written digits has $d = 28 \times 28 = 784$ pixels, for each of which, the grey scale is codified in an integer x_a in the range $[0, 255]$. Nearby pixels have typically similar values of x_a , hence $p(\mathbf{x})$ should be a model of strongly interacting variables.

We focus on stochastic models, such as Restricted Boltzmann Machines (RBM) or Deep Belief Networks (DBN), with a finite number of discrete internal states. The goal of learning is to find a statistical model $p(\mathbf{s})$ over a discrete variables \mathbf{s} , and a mapping $p(\mathbf{x}|\mathbf{s})$ from \mathbf{s} to \mathbf{x} , such that the generating distribution

$$p_{\text{gen}}(\mathbf{x}) = \sum_{\mathbf{s}} p(\mathbf{x}|\mathbf{s})p(\mathbf{s})$$

is as close as possible to the empirical one (in unsupervised learning), or that the representation approximates a functional relation $\underline{x}_{\text{out}} = f(\underline{x}_{\text{in}})$ between two parts of the data $\mathbf{x} = (\underline{x}_{\text{in}}, \underline{x}_{\text{out}})$ as well as possible (in supervised learning). The objective function employed may differ, yet in both cases the aim is that of approximating the unknown generative process $p(\mathbf{x}) \approx p_{\text{gen}}(\mathbf{x})$ as closely as possible (or at least that part which is responsible for the dependence of the labels $\underline{x}_{\text{out}}$ on the

input $\underline{x}_{\text{in}}$). Here we focus on the outcome of this process, abstracting from algorithmic details on how the representation is learned.

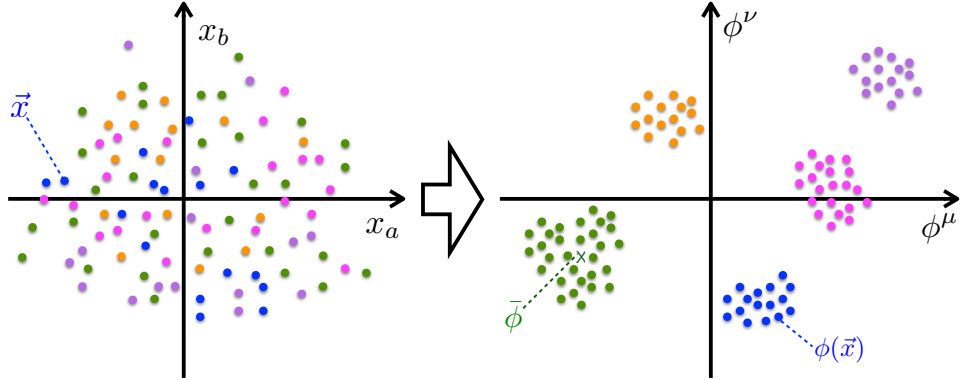


Figure 1: Sketch of the map of a dataset to the space of features. Points with similar features $\phi(\mathbf{x}) \approx \bar{\phi}$ are statistically identical. Statistically distinct points are distinguished by a significant variation $\delta\phi$ of the feature vector.

Let us assume that the structure of dependencies in $p(\mathbf{x})$ can be represented in terms of a vector of hidden features $\phi = (\phi^1, \dots, \phi^m)$, as shown in Fig. 1, so that *i*) points with a similar value $\phi(\mathbf{x}) \approx \bar{\phi}$ correspond to statistically undistinguishable points in the data, and *ii*) the variation $\delta\phi$ captures the variability across qualitatively different points \mathbf{x} .

Let us relate this picture to the properties of a representation $p(\mathbf{s})$ at a given resolution $H[\mathbf{s}]$. Features can be defined in terms of a vector of functions $\phi(\mathbf{s})$ defined on the states \mathbf{s} of the machine, as

$$\phi(\mathbf{x}) = \sum_{\mathbf{s}} \phi(\mathbf{s}) p(\mathbf{s}|\mathbf{x}). \quad (3)$$

Note that $p(\mathbf{s}|\mathbf{x})$ depends on the unknown distribution $p(\mathbf{x})$ and so does $\phi(\mathbf{x})$, instead $\phi(\mathbf{s})$ is defined in terms of the representation \mathbf{s} , so it is in principle accessible.

In the representation space \mathbf{s} , the picture in Fig. 1 translates in the decomposition

$$p(\mathbf{s}) = \int d\bar{\phi} p(\mathbf{s}|\bar{\phi}) p(\bar{\phi}) \quad (4)$$

where $p(\mathbf{s}|\bar{\phi})$ is such that¹

$$\sum_{\mathbf{s}} \phi(\mathbf{s}) p(\mathbf{s}|\bar{\phi}) = \bar{\phi}. \quad (5)$$

The requirement *i*) implies that the conditional distribution $p(\mathbf{s}|\bar{\phi})$ should contain no useful information or, conversely, that the expected values $\bar{\phi}$ contains all useful information to determine

¹Note that $\bar{\phi}$ is the same in both representations. Indeed, given the distribution $p(\mathbf{x}|\bar{\phi})$ of all points with $\phi(\mathbf{x}) \approx \bar{\phi}$, as long as $\int d\mathbf{x} \phi(\mathbf{x}) p(\mathbf{x}|\bar{\phi}) = \bar{\phi}$, one recovers Eq. (5) using Eq. (3) and $p(\mathbf{s}|\bar{\phi}) = \int d\mathbf{x} p(\mathbf{s}|\mathbf{x}) p(\mathbf{x}|\bar{\phi})$.

$p(\mathbf{s}|\bar{\phi})$. The maximum entropy principle implies that²

$$p(\mathbf{s}|\bar{\phi}) = \frac{1}{Z(g(\bar{\phi}))} e^{\sum_{\mu=1}^m g^{\mu}(\bar{\phi})\phi^{\mu}(\mathbf{s})}, \quad (6)$$

where $g^{\mu}(\bar{\phi})$ is fixed by the constraint in Eq. (5). In information theoretic terms, $\phi(\mathbf{s})$ are the minimal sufficient statistics of $p(\mathbf{s}|\bar{\phi})$. A consequence of Eq. (6) is that, all points \mathbf{s} with the same features $\phi(\mathbf{s})$ have the same probability, or equivalently, the energy

$$E_s = -\log \int d\bar{\phi} \frac{p(\bar{\phi})}{Z(g(\bar{\phi}))} e^{\sum_{\mu} g^{\mu}(\bar{\phi})\phi^{\mu}(\mathbf{s})} = \mathcal{E}(\phi(\mathbf{s})) \quad (7)$$

must be a function of $\phi(\mathbf{s})$. In other words, the statistical dependence of the variables can be represented as the Markov chain³

$$\mathbf{x} \rightarrow \mathbf{s} \rightarrow \phi \rightarrow E. \quad (8)$$

The data processing inequality [18] then implies that

$$I(\mathbf{s}, \phi) \geq I(\mathbf{s}, E) = H[E], \quad (9)$$

where the last equality comes from the fact that $I(\mathbf{s}, E) = H[E] - H[E|\mathbf{s}]$ and $H[E|\mathbf{s}] = 0$. Therefore, $H[E]$ provides a lower bound to the information that the representation extracts on the hidden features. Machines with a maximal relevance $H[E]$, at a fixed resolution $H[\mathbf{s}]$, push this lower bound as much as possible thereby achieving maximally informative representations.

The relation (8) also implies that $I(\mathbf{s}, \phi) \geq I(\mathbf{x}, \phi)$, where the equality holds when the internal state \mathbf{s} of the learning machine is a deterministic function $\mathbf{s}(\mathbf{x})$ of the data. Interestingly, the *clamped* distribution $p(\mathbf{s}|\mathbf{x})$ of learning machines such as RBMs or DBNs in hidden layers with good generating capacity, is highly peaked on a single state $s(\mathbf{x})$, i.e. it is close to being deterministic (see also Sect. 4). So when the internal state \mathbf{s} of the learning machine is a deterministic function $\mathbf{s}(\mathbf{x})$ of the data, then the relevance $H[E]$ provides also a lower bound on the information that the data contains on the features.

Notice that $H[\mathbf{s}|\phi]$ provides a measure of that part of $H[\mathbf{s}]$ which is not informative on the features. By Eq. (9), this is upper bounded by $H[\mathbf{s}|E]$. Maximising $H[E]$ at fixed resolution $H[\mathbf{s}]$ implies minimising $H[\mathbf{s}|E] \geq H[\mathbf{s}|\phi]$, i.e. squeezing noise out of the representation.

An alternative definition of OLM, are machines that extract the most compressed representations from data, at a minimal information content $H[E]$ on the features

$$\min_{I(\mathbf{s}, \phi) \geq H[E]} H[\mathbf{s}]. \quad (10)$$

3 Learning Machines with discrete energy levels

The aim of this Section is to investigate the principle of maximal relevance for a specific class of models in order to shed light on the properties of OLM. We shall consider fully connected models of

²It's interesting to remark, in passing, the similarity of Eq. (6) with models discussed in [17]. [17] show that hidden variables in statistical models generate Zipf's law. The occurrence of Zipf's law in RBMs [7] is a natural manifestation of this observation, in the present framework.

³The notation $z \rightarrow y \rightarrow w$ implies that, if y is known, w and z are independent, i.e. that $I(z, w|y) = 0$ [18]. This holds trivially true if w is a function of y , because then w is not a random variable, when y is known.

Ising spin, with couplings $J_{i,j} = \pm J$. These are not particularly efficient as learning machines, but they provide a well defined playground for investigating the properties that make some architectures more efficient (i.e. with a larger $H[E]$) than others. This also allows us to contrast the properties of models with large $H[E]$ with those of well known models, such as the mean field Ising ferromagnet and the $J_{i,j} = \pm J$ spin glass. Finally, for this class the energy levels belong to a discrete set, which makes the analysis particularly convenient and transparent.

3.1 The optimal Ising learning machine

We consider a model of n spins $\mathbf{s} = (s_1, \dots, s_n)$, $s_i = \pm 1$, defined by an Hamiltonian

$$\mathcal{H}(\mathbf{s}) = - \sum_{i < j} J_{i,j} s_i s_j, \quad (11)$$

where the couplings take values $J_{i,j} \in \{\pm J\}$. This induces a Gibbs measure

$$p(\mathbf{s}) = \frac{1}{Z} e^{-\mathcal{H}(\mathbf{s})}, \quad Z = \sum_{\mathbf{s}} e^{-\mathcal{H}(\mathbf{s})}, \quad (12)$$

on the space of configurations. As discussed above, we define the energy as the coding cost $E_{\mathbf{s}} = -\log p(\mathbf{s}) = \mathcal{H}(\mathbf{s}) + \log Z$, and address the optimisation problem

$$\mathcal{J} = \arg \max_{\hat{J}: H[\mathbf{s}] = \bar{E}} H[E], \quad (13)$$

where the maximum is taken over all matrices with elements $J_{i,j} = \pm J$, and on \hat{J} . \mathcal{J} is the subset of such matrices that achieve a maximal value of $H[E]$ ⁴.

In order to compute $H[E]$ as a function of \hat{J} , we define the distribution of the energy as

$$p(E) = \sum_{\mathbf{s}} p(\mathbf{s}) \delta(E - E_{\mathbf{s}}) = W(E) e^{-E} \quad (15)$$

where $W(E)$ is the number of states \mathbf{s} with energy $E_{\mathbf{s}} = E$. From this and Eq. (2), we compute the value of $H[E]$.

The rest of this section is devoted to describe the trade-off between $H[E]$ and $H[\mathbf{s}]$ for models in the class of Eq. (11). Since $H[\mathbf{s}] \leq n \log 2$ within this class, we shall discuss the rescaled resolution

$$h_s = \frac{H[\mathbf{s}]}{n \log 2}. \quad (16)$$

⁴We remark that this is a dual problem with respect to that addressed in statistical physics. The physical properties of a system with Hamiltonian $E_{\mathbf{s}}$ are derived, from the maximum entropy principle, i.e. finding the distribution $p(\mathbf{s})$ over microscopic states \mathbf{s} that maximises the entropy $H[\mathbf{s}]$ at a given value of the average energy $\langle E \rangle = \sum_{\mathbf{s}} p(\mathbf{s}) E_{\mathbf{s}} = \bar{E}$. As a result, the distribution over the set of 2^n configurations is

$$P(\mathbf{s}) = \frac{1}{Z} e^{-\beta E_{\mathbf{s}}}, \quad Z = \sum_{\mathbf{s}} e^{-E_{\mathbf{s}}} \quad (14)$$

with Z being the partition function and β is adjusted to satisfy the constraint $\langle E \rangle = \bar{E}$. Typical states drawn from $p(\mathbf{s})$ have all the same energy $E_{\mathbf{s}} \approx \bar{E}$. By contrast, in OLM the maximisation is carried out over the Hamiltonian at fixed entropy $H[\mathbf{s}]$, with $p(\mathbf{s}) = e^{-E_{\mathbf{s}}}$.

Analogously, we observe that E_s/J takes values only on the integers and $|E_s|/J \leq n(n-1)/2$. This justifies the introduction of the rescaled relevance

$$h_E = \frac{H[E]}{\log n} \quad (17)$$

that takes values in the interval $[0, 2]$. The sub-extensive nature of $H[E]$ suggests that properties that contribute to the relevance of a model may not be accessible to saddle point analysis of the partition function, that focuses only the leading extensive terms. The behaviour of $H[E]$ with the number n of spins depends on the fact that the model (11) depends only on one parameter J^5 .

The information content of a model can be quantified in terms of the Stochastic Complexity in Minimum Description Length [19]. This is given by

$$\text{SC} = \int d\theta \sqrt{\det \hat{F}(\theta)}, \quad (18)$$

where $\hat{F}(\theta)$ is the Fisher information matrix and θ is the vector of parameters. Our models depend only on one parameter J and the Fisher information coincides with the variance of the variable $\mathcal{H}(s)/J$, which is closely related to the specific heat.

A second measure of the information content of a model can be obtained by the area under the h_E vs h_s curve. This scores models according to their relevance across different levels of resolution. We shall call this measure Multi-Scale Relevance (MSR), following [20], that introduced a similar measure on single samples.

Both h_s and h_E only depend on \hat{J} through the degeneracy $W(E)$ of energy levels. $W(E)$ is invariant under the permutation of the spins. Hence if $\hat{J} \in \mathcal{J}$ then also the matrix with elements $J_{\pi(i),\pi(j)}$ is a solution, where $\pi(i)$ is a permutation of the indices $i = 1, \dots, n$. Also, matrices \hat{J} and \hat{J}' that are related by a gauge symmetry $J'_{i,j} = \tau_i J_{i,j} \tau_j$, with $\tau_i = \pm 1$, have the same $W(E)$. Hence, if $\hat{J} \in \mathcal{J}$, then also its gauge transformed \hat{J}' belongs to \mathcal{J} . We partially exploit these symmetries by fixing the gauge with the choice $J_{1,j} = 1$ for all $j \neq 1$. Henceforth we shall focus on the reduced set \mathcal{J} of matrices with this choice of the gauge.

An interesting point that we shall discuss is how the set \mathcal{J} of solutions \hat{J} are organised, i.e. whether they correspond to isolated maxima or whether they form a compact set of nearby solutions in terms of local moves that involves the change of few $J_{i,j}$'s. This may shed light on the accessibility of solutions of Eq. (13) to learning rules such as stochastic gradient descent.

3.2 Exact enumeration for small systems

Each model in Eq. (11) is defined by a choice of the sign of the $n(n-1)/2$ couplings $J_{i,j}$ and by the strength J of the couplings. There are $2^{n(n-1)/2}$ possible ways of choosing the signs. Yet, this number can be reduced by fixing the gauge. We were able to compute h_E as a function of h_s for all models up to $n = 9$ spins. This allows us to find those models that achieve a maximal h_E for a given resolution h_s .

Representative results are shown in Fig. 2 for $n = 8$. There are $M = 219$ different curves in the left panel, each corresponding to a different degeneracy $W(E)$ of energy levels⁶. Fig. 2(left)

⁵For example, in a model with $\mathcal{H}(s) = -\sum_{i < j} J_{i,j} s_i s_j - \sum_i h_i s_i$, $J_{i,j} = \pm J$ and $h_i = \pm h$, the energy takes values on a set of point $E = Jn_J + hn_h$ with $n_J \in [-n(n-1)/2, n(n-1)/2]$ and $n_h \in [-n, n]$. So the number of possible values of E grows at most as n^3 , and we expect the $h_E \in [0, 3]$. This suggests that $H[E]$ grows in general with $\log n$, with a coefficient that is bounded by a constant that grows linearly with the number of parameters.

⁶For $n = 3, 4, 5, 6, 7, 8$ and 9 , we find $M = 2, 3, 7, 16, 54, 219$ and 1625 , respectively.

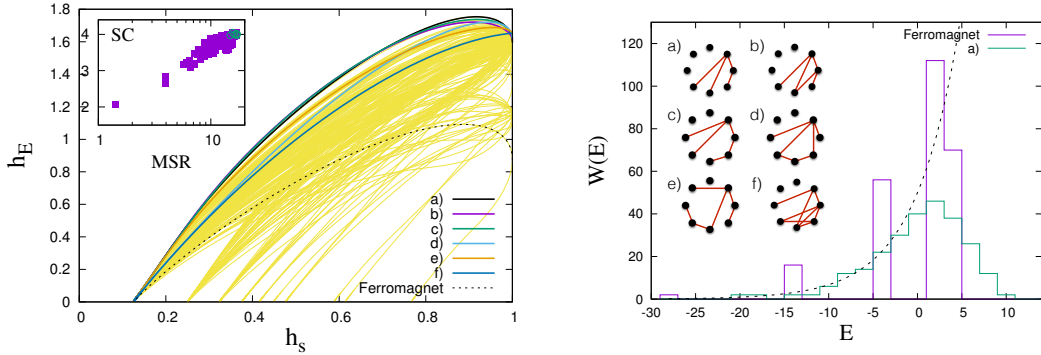


Figure 2: (Left) h_E vs h_s for all models with $n = 8$ spins. The curves highlighted correspond to the models shown on the right plot (only $J_{i,j} < 0$ are shown as red links). The dotted line corresponds to the ferromagnet. The inset reports the relation between the stochastic complexity (SC) and the Multi-Scale Relevance (MSR), which is the area under the h_E vs h_s curve. The points corresponding to the models highlighted in the main plot are shown in green. (Right) Degeneracy $W(E)$ of energy levels for the model $a)$ (top left) and for the ferromagnet. The dotted line corresponds to an exponential $W(E) = W_0 e^{\nu E}$ with $\nu = 0.2$.

shows, in particular, the six functions h_E that achieve maximal relevance for some value of h_s . A representative choice of the corresponding matrix $\hat{J} \in \mathcal{J}$ is shown in the right part of Fig. 2. We remark that there are many models with the same $W(E)$, that cannot be reduced to one another by a permutation of the spins (for model $a)$ there are 325 different models). Fig. 2(right) shows the degeneracy $W(E)$ for model $a)$ (top left in Fig. 2 right). As a comparison, Fig. 2 also shows the curve $h_E(h_s)$ (left) and the degeneracy $W(E)$ for the ferromagnet ($J_{i,j} = J \forall i, j$).

The architectures that achieve maximal relevance, that we identify with OLM, have the following distinctive properties: *i)* the large majority of the couplings $J_{i,j}$ are positive, which means that OLM are close to ferromagnetic models. Indeed, the ground state of all OLM are the same as that of the ferromagnet. Yet, *ii)* the relevance for OLM achieves a much higher value than that of the ferromagnetic model (dotted line in Fig. 2 left). This is consistent with the fact that the degeneracy for the ferromagnet is concentrated on few values of E , whereas for OLM it spreads over a larger number of values of E . The degeneracy $W(E)$ is consistent with an exponential behaviour, as predicted in [13]. Finally *iii)* the architectures of OLM appear to be rather inhomogeneous, with negative $J_{i,j}$ impinging on a small subset of nodes. Such a low degree of symmetry, may be the origin of the fact that the number $|\mathcal{J}|$ of matrices \hat{J} that share the same $W(E)$ of OLM is rather large (see Table 1).

It is interesting to analyse how the set \mathcal{J} is structured with respect to a single rewiring of a negative $J_{i,j}$, because this may shed light on the accessibility of OLM under a local learning dynamics during training. We find (see Table 1 for $n = 8$) that the multiplicity of these sets decreases with the value of h_s for which these OLM are optimal. These sets are dominated by a single largest component which is suggestive of the wide flat minima discussed in [6]. This observation is corroborated by the fact that any $OLM \in [a, b, \dots, f]$ can be obtained by a different OLM by local

OLM	$ \mathcal{J} $	connected components	h_s
f	80640	80640×1	$[0.999, 1]$
e	40320	$35280 \times 1 + 5040 \times 1$	$[0.995, 0.999]$
d	10080	10080×1	$[0.984, 0.995]$
a	3360	$2940 \times 1 + 12 \times 35$	$[0.71, 0.984]$
c	10080	$7560 \times 1 + 1260 \times 1 + 12 \times 105$	$[0.62, 0.71]$
b	3360	$2100 \times 1 + 420 \times 2 + 4 \times 105$	$[0.22, 0.62]$

Table 1: Structure of the set of \hat{J} corresponding to the OLM in Fig. 2 (right). The second column yields the size of the set \mathcal{J} of matrices \hat{J} that achieve maximal h_E in a given interval (4th column). The third column lists the connected components in \mathcal{J} under rewiring of a single negative coupling. The format used is size \times multiplicity + All models in the same class share the same (ferromagnetic) ground state.

moves, such as the addition and/or the rewiring of a single negative $J_{i,j}$. As h_s decreases, we see a tendency of the set to shrink and to fragment in different connected components.

Finally, the inset of Fig. 2 left) shows that the Stochastic Complexity (SC) of a model generally increases with the Multi-Scale Relevance (MSR) introduced above, even though there are deviations from a simple functional behaviour.

3.3 Some particular architectures

This section analyses specific architectures for which the curve $h_E(h_s)$ can be computed for large values of n . We start with the ferromagnet, that although far from an optimal architecture, will serve as a benchmark.

3.3.1 The mean field Ising ferromagnet and spin glasses

The mean field Ising ferromagnet (MFIFM) corresponds to $J_{i,j} = J$ for all i, j . For large n , this is characterised by a high temperature disordered phase for $J < J_c/n$ and by a low temperature ordered phase for $J > J_c/n$ where a non-zero magnetisation spontaneously appears. Notice that the values of the energy for the MFIFM range over an interval $[-Jn(n-1)/2, Jn(n-1)/2]$ of order n^2 , but energies $E_{\mathbf{s}}$ can take at most $n+1$ different values

$$E_m = -\frac{J}{2}(m^2 - n), \quad m = \sum_{i=1}^n s_i = -n, -n+2, \dots, n-2, n. \quad (19)$$

This implies that $h_E \leq \log(n+1)/\log n$. Note also that there is a single matrix \hat{J} which corresponds to the degeneracy of energy levels $W(E)$ of the MFIFM.

Fig. 3 reports the curves $h_E(h_s)$ for several values of n . The curve exhibits a maximum in the neighbourhood of the critical point $J \approx J_c/n$. The decreasing part to the right of the maximum corresponds to the high temperature phase, whereas the one to the left of the maximum to the low temperature phase. As n increases, the maximum shifts to values of h_s closer and closer to one. At the same time, the maximum gets sharper and sharper and its value slowly decreases towards a finite limit (see inset).

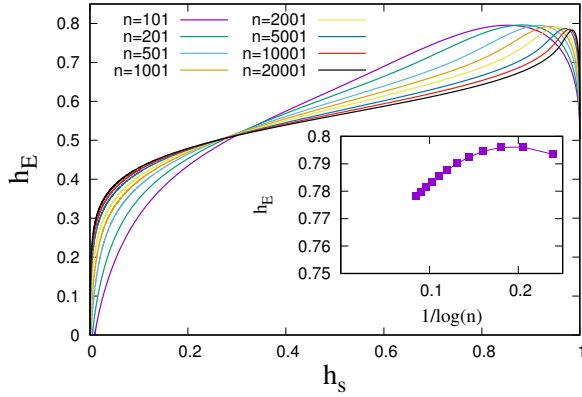


Figure 3: h_E vs h_s for the MFIFM for $n = 101, 201, 501, 1001, 2001, 5001, 10001$ and 20001 . Inset: maximal value of h_E as a function of $1/\log n$.

The limiting form of the curve $h_E(h_s)$ can be computed in the limit $n \rightarrow \infty$ (see Appendix). This shows that

$$\lim_{n \rightarrow \infty} h_E = \begin{cases} 1/2 & J \neq J_c/n \\ 3/4 & J = J_c/n, \end{cases} \quad (20)$$

which is consistent with the bound $h_E \leq 1$. The analysis leading to this result (see Appendix) confirms that h_E depends on sub-leading contributions that arise from the integration of fluctuations around the saddle point value. At the critical point $J = J_c/n$, the resolution converges to $h_s \rightarrow 1$. On the other hand, for $J = 0$ we have $h_s = 1$ and $h_E = 1/2$, exactly. Hence depending on how $h_s \rightarrow 1$, all values of $h_E \in [1/2, 3/4]$ can be achieved. Fig. 3 is fully consistent with this result, although the convergence is very slow. Notice also that the limiting value is approached from above for some values of h_s and from below for other values.

When $J_{i,j} = \pm J$ are chosen at random with equal probability, we know that the relevant scale for J is $1/\sqrt{n}$. The ground state energy is extensive so E_S spans a number of energy levels that is at most of order $n^{3/2}$. Therefore we expect that $h_E \leq 3/2$ for a spin glass. In fact, for $J = c/\sqrt{n}$ with c finite but different from the critical point, the distribution of the energy extends over a range of order $\delta E \propto \sqrt{n}$. This suggests that the number of energy levels on which $p(E)$ is non-zero grows linearly with n , and hence that $h_E \rightarrow 1$ as $n \rightarrow \infty$ for a model with randomly chosen $J_{i,j}$.

3.3.2 The star model

Let us now consider a model that differs from a MFIFM by that fact that one spin has antiferromagnetic interactions with $\ell < n$ other spins. More precisely, $J_{i,j} = -1$ if $i = 1$ and $j \leq \ell + 1$, and $J_{i,j} = +1$ otherwise. We divide the $n - 1$ group of spins, except spin s_1 , into two groups: the ℓ ones with anti-ferromagnetic interaction with s_1 and the remaining $n - \ell - 1$. If q and k are the number of positive spins in the first and second group, respectively, the energy is given by

$$\epsilon(k, q, s_1) = J \left[s_1(n - 1 - 2\ell - 2k + 2q) - \frac{1}{2} (2k + 2q - n + 1)^2 + \frac{n - 1}{2} \right]. \quad (21)$$

The degeneracy of energy levels is given by

$$W(E) = \sum_{k=1}^{n-1-\ell} \sum_{q=1}^{\ell} \sum_{s_1=\pm 1} \binom{\ell}{q} \binom{n-1-\ell}{k} \delta_{E, \epsilon(k, q, s_1)}. \quad (22)$$

Notice that for $\ell = 0$ one recovers the MFIFM. A gauge transformation $J_{i,j} \rightarrow \tau_i J_{i,j} \tau_j$, with $\tau_1 = -1$ and $\tau_i = +1$ for $i > 1$, maps a model with $\ell > n/2$ into a model with $\ell' = n - \ell \leq n/2$. So it is sufficient to study the model for $\ell \leq n/2$.

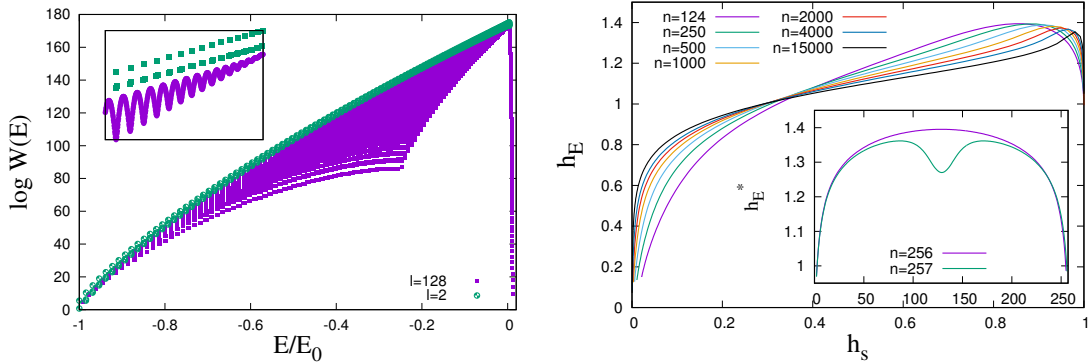


Figure 4: (Left) Degeneracy of energy levels for $n = 256$ and $\ell = 2$ and 128 . Energies are rescaled by $E_0 = Jn(n-1)/2$. For $\ell = 2$ there are 385 distinct energy levels, whereas for $\ell = 128$ there are 8511. The inset magnifies the data in the range $E \in [-0.03E_0, 0]$. (Right) curves $h_E(h_s)$ for $\ell = n/2$ (full lines) and different values of n . Inset: maximal (over h_s) value of h_E as a function of ℓ , for $n = 256$ and 257 .

The degeneracy $W(E)$ of energy levels is shown in Fig. 4(left) for $n = 256$, $\ell = 2$ and $\ell = 128$. As ℓ increases, the number of different values that E takes also increases. For $n = 256$, the values that E can take are 129, 385 and 8511 for $\ell = 0, 2$ and 128 , respectively. Indeed, for the MFIFM ($\ell = 0$) E can take only $n/2 + 1$ different values (for even n), whereas for $\ell = n/2$ we find that the number of possible values of E grows almost as n^2 . At the same time, $W(E)$ acquires a rapid variation as a function of E , so that for large n , $W(E)$ becomes a space filling curve (see Fig. 4 left and inset). Interestingly, the thermodynamics of the model is dominated by the convex envelope of $\log W(E)$, which is the same as that of the MFIFM. Therefore the star model and the MFIFM have indistinguishable thermodynamic properties. This is consistent with the fact that the number of $J_{i,j} = -1$ is a fraction of order $1/n$ of the total number of interactions and that they impinge on one out of the n spins. It is easy to check that, for $\ell \leq n/2$, the ground state of the star model is the ferromagnetic state $s_i = s_j$ for all $i \neq j$.

The maximal value of $h_E^*(\ell) = \max_{h_s} h_E$ for even values of n is achieved at $\ell = n/2$ (see inset of Fig. 4 right), whereas for odd values of n , h_E^* reaches a lower maximum at $\ell \approx n/3$. The symmetry for $\ell \rightarrow n - \ell$ of these curves is a consequence of the gauge transformation discussed above. The curves $h_E(h_s)$ for $\ell = n/2$ and for different values of n are shown in Fig. 4(right). We find that the highest relevance $H[E]$ for even n and $\ell = n/2$, grows faster than $\log n$. An extrapolation of the maximal value of h_E is consistent with $h_E \rightarrow 5/4$ as $n \rightarrow \infty$. At fixed values of h_s instead, we

observe a slower growth of $H[E]$ with $\log n$, that may be consistent with $h_E \rightarrow 1$ for large n . These values are consistent with the fact that, the degeneracy of each energy level E_m of the MFIFM is spread over n other energy levels, \sqrt{n} of which contribute to $H[E]$ (see inset of 4 left). This suggests a relation $h_E^{\text{Star}} = h_E^{\text{MFIFM}} + 1/2$, that is consistent with our numerical results.

Finally we remark that the set of models with this structure is decomposed into n subsets, each of which is connected with respect to a single rewiring of a negative $J_{i,j}$. Indeed each of the ℓ negative links can be rewired to any of the $n - \ell - 1$ spins with all ferromagnetic interactions. This dynamics, however, keeps the hub node fixed, so each of the n possible choices of the hub identifies a connected component. This is consistent with the conjecture that models with high relevance are organised in sets easily accessible by local update dynamics.

3.3.3 A recursive model

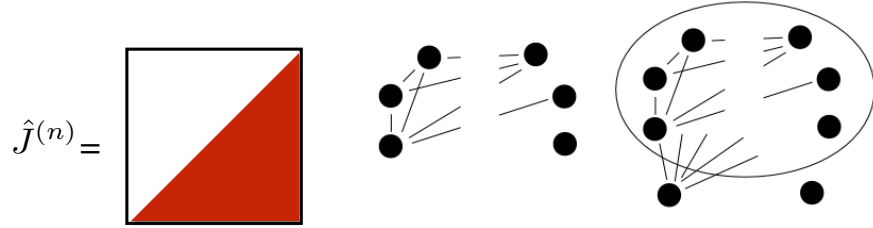


Figure 5: Left: Sketch of the structure of the matrix \hat{J} for structure of recursive models for $\ell = 1$. Red indicates negative $J_{i,j}$. Right: sketch of the recursion that relates a model with n spins to a model with $n + 2$ spins.

The next architecture that we shall consider is one where $J_{i,j} = -1$ for $i > \ell$ and $j > n + \ell - i$, and $J_{i,j} = +1$ otherwise. For $\ell = 1$ this corresponds to a matrix \hat{J} that has the form shown in Fig. 5(left). In these models, the set of negative $J_{i,j}$ is organised according to a nested network [21]. These matrices can be obtained through a recursive procedure (see Fig. 5 right): we start from $n = 2$ with $J_{1,2} = +1$. At each iteration, from a system of n spins, we add two spins, s_0 and s_{n+1} . The spin s_0 has $J_{0,j} = -1$ with all other spins $j \leq n$. The spin s_{n+1} has $J_{i,n+1} = +1$ with all spins, including s_0 . This generates a matrix with $n + 2$ spins with the desired structure⁷.

It is possible to generalise the recursion relation to obtain matrices with different values of ℓ . For example, the case $\ell = n/2$ can be obtained by separating the set of spins into two equal parts,

⁷ For each state at energy E and magnetisation $M = \sum_{i=1}^n s_i$, and each choice of s_0, s_{n+1} , we obtain a state of the system with $n + 2$ spins with energy

$$E' = E - J[s_0 s_{n+1} - s_0 M + s_{n+1} M] \quad (23)$$

and magnetisation $M' = M + s_0 + s_{n+1}$. Thus the energy degeneracy of a system of n spins can be computed as $W_n(E) = \sum_M w_n(E, M)$, where w_n satisfies the recursive equation

$$w_{n+2}(E', M') = \sum_{s_0, s_{n+1}=\pm 1} \sum_{E, M} w_n(E, M) \delta_{E'(E)} \delta_{M', M+s_0+s_{n+1}}. \quad (24)$$

Here the shorthand $\delta_{E'(E)}$ reduces the sum to only those terms where Eq. (23) is satisfied.

$\mathcal{I}_\leq = \{i \leq n/2\}$ and $\mathcal{I}_> = \{i > n/2\}$. To each of the two sets we add two spins at each iteration, thereby obtaining a system with $n+4$ spins. Of the two spins added to \mathcal{I}_\leq , one has $J_{0,j} = -1$ with all spins $j \in \mathcal{I}_\leq$ and $J_{0,j} = +1$ for all $j \in \mathcal{I}_>$. The other three spins have ferromagnetic interactions with all other spins, as well as among themselves. It is easy to see by induction, that the ground state of this model is the ferromagnetic one $s_i = s_j$ for all i, j . This holds true for all $\ell \leq n/2$.

Numerical iteration of the recursion relations allowed us to compute the degeneracy $W_n(E)$ and the curves $h_E(h_s)$ for different values of n and ℓ . Fig. 6 shows the results for different values of n and for $\ell = 1$ (left) and $\ell = n/2$ (right).

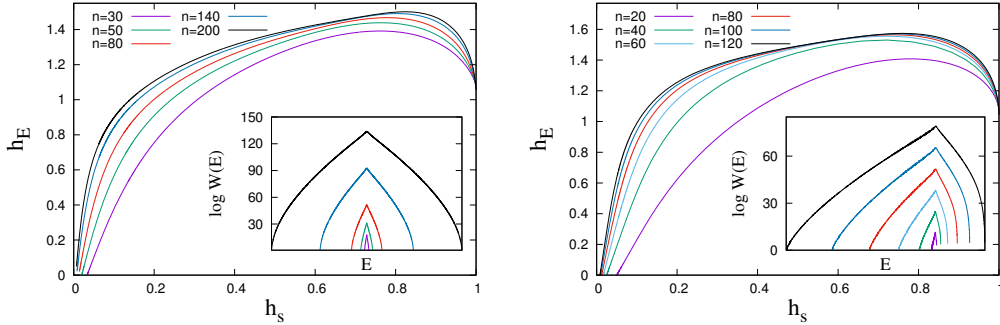


Figure 6: Relevance h_E as a function of h_s for the recursive model with $\ell = 1$ (left) and $\ell = n/2$ (right), for different values of n (see legend). The inset shows the degeneracy $\log W(E)$ as a function of E for the corresponding models.

Although we could not access values of n as large as in the previous cases, Fig. 6 shows that this model has qualitatively distinct features. First, we found that $\log W(E)$ approaches a continuous function of E and it has support on a number of energy levels that increases as n^2 . For $\ell = 1$ we found that $W(E) = W(-E)$ is a symmetric function of E (see inset, left). Second, in both cases, we found that h_E increases monotonically with n and it approaches a limiting value already for relatively small values of n . The maximal limiting values of h_E is higher than that achieved with the other architectures. We note that the number of anti-ferromagnetic interactions in these models is proportional to n^2 , and hence their thermodynamic properties in the $n \rightarrow \infty$ limit differ from those of the MFIFM.

For a given value of ℓ , there are $\frac{n!}{(n-\ell)!}$ possible models depending on how the set of $n-\ell$ fully ferromagnetic spins are chosen and on the ranking of the ℓ spins. This set of models forms a single connected component under a single rewiring of a $J_{i,j} = -1$ ⁸, which is again consistent with the conjecture that OLM are easily accessible by local updates of the couplings.

⁸In order to show this, let ∂_i be the set of spins with $J_{i,j} = -1$. If we sort spins in such a way that $\delta_1 = (1, \dots, \ell)$, $\delta_2 = (1, \dots, \ell-1), \dots, \delta_k = (1, \dots, \ell-k+1), \dots$, then the rewiring of the link $(k, \ell-k+1)$ to $(k+1, \ell-k+1)$ interchanges the order of spins k and $k+1$ in the hierarchy. The rewiring of the link $(1, \ell)$ to $(1, k)$ with $k > \ell$ changes the membership of spins in the network connected by $J_{i,j} = -1$. Repeated application of these two moves in the appropriate order makes it possible to reach any model in the set from any other model.

3.4 A numerical experiment

The results in the previous sections suggest that the optimisation of the likelihood for a given dataset will converge more likely to models that afford a richer description of the data generating process, provided the data contains a rich statistical structure. Our prediction is that these models are those with the highest relevance $H[E]$. In order to test this prediction, we compared the ability of models with different matrices \hat{J} to represent a dataset.

Because of the exponential growth⁹ in the number of models with the number n of spins, we limit our analysis to the case $n = 5$. There are seven different classes of models (see Table 2). Each class contain models with the same $W(E)$ and hence with the same curve $h_E - h_s$. The class that achieves maximal value of $H[E]$ in a wide range of $H[\mathbf{s}]$, that we shall call class A, contains two models¹⁰. Class A also has the largest values of the SC and of the MSR. The other classes – that we call B, C, D, E, FM and AF – contain one (E, AF and FM) or two models (B, C and D). Class FM contains the ferromagnetic model and AF the anti-ferromagnetic one.

Model	MSR	SC	$J_{i,j} < 0$
FM	4.176	2.768	-
A	4.771	2.919	$\{(1, 2)\}, \{(1, 2), (1, 3), (1, 4)\}$
B	3.037	2.595	$\{(1, 2), (1, 3)\}, \{(1, 2), (1, 2), (2, 3), (3, 4)\}$
C	1.510	2.154	$\{(1, 2), (1, 3), (2, 3)\}, \{(1, 2), (1, 3), (1, 4), (2, 3), (2, 4)\}$
D	3.656	2.861	$\{(1, 4), (2, 3)\}, \{(1, 2), (1, 3), (1, 4), (2, 3)\}$
E	1.329	2.022	$\{(1, 2), (1, 3), (1, 4), (2, 3), (2, 4), (3, 4)\}$
AF	0.310	1.356	all

Table 2: The seven classes of models for $n = 5$ spins. The last column lists the values (i, j) for which $J_{i,j} < 0$. Some of the classes (FM, AF and E) correspond to a single model, the others to two. The second and third column lists the values of the MSR and SC respectively.

We focus on two datasets of $m = 9$ binary variables $\mathbf{x} \in \{0, 1\}^m$. One is that used in [22] on the voting patterns in the US Supreme Court. This reports the votes (in favour or against) of the $m = 9$ judges of the US Supreme Court for $N = 895$ cases. The second is obtained from the MNIST dataset [16], focusing on a patch of 3×3 pixels of the $N = 6 \cdot 10^4$ hand written digits¹¹, as in [7]. The joint distribution is built by taking $p(\mathbf{s})$ as in Eqs. (11,12) and

$$p(\mathbf{x}|\mathbf{s}) = \frac{1}{Q_{\mathbf{s}}} \exp \left[\sum_{j=1}^m \left(b_j + \sum_{i=1}^n s_i w_{i,j} \right) x_j \right], \quad Q_{\mathbf{s}} = \prod_{i=1}^m \left[1 + e^{b_j + \sum_i s_i w_{i,j}} \right]. \quad (25)$$

For every model and each value of J we maximise the log-likelihood over the parameters \vec{b} and \hat{w} by gradient ascent. Fig. 7 shows that over a wide range of resolutions, the maximum of the

⁹To give an idea of the combinatorial explosion of the class of models, for $n = 8$ there are 219 different classes, each with many distinct models that cannot be reduced one to the other by a gauge transformation or by a permutation of the spins. For example, there are 325 models with the same $H[E] - H[\mathbf{s}]$ curve as model a in Fig. 2.

¹⁰One with only one negative coupling and the other with three negative couplings incident on the same node, e.g. $J_{1,2} = J_{1,3} = J_{1,4} < 0$.

¹¹Each MNIST data point contains 28×28 pixels, with an integer value in the range $[0, 255]$. We first transform the dataset into coarse grained pixels of 2×2 original pixels, and binarise the result applying a threshold. Then we focus on the 3×3 patch with pixels coordinates (i, j) ranging from 5 to 7.

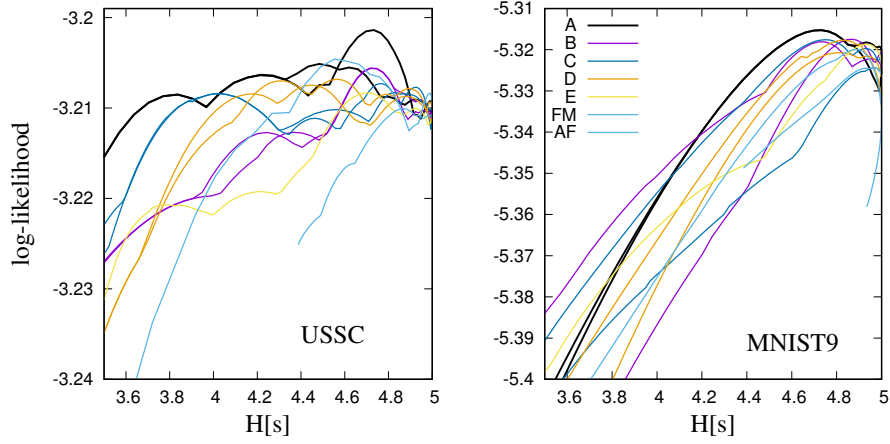


Figure 7: Log likelihood for the USSC (left) and MNIST9 data for models of $n = 5$ spins, as a function of $H[\mathbf{s}]$. Models are classified according to their $h_E - h_s$ curve (see Table 2).

likelihood is attained for models in class A. In particular, this interval contains the point where the log-likelihood achieves its maximum.

4 Learning Machines with continuous energy levels

The analysis of the previous Section can be generalised for learning machines with energy levels $E_{\mathbf{s}}$ that belong to a continuum spectrum. We shall focus on the architecture of Restricted Boltzmann Machines (RBM). These have n_v visible units $\mathbf{x} = (x_1, \dots, x_{n_v})$, and n hidden binary units $\mathbf{s} = (s_1, \dots, s_n)$ with $s_i = 0, 1$. The joint probability distribution is

$$p(\mathbf{x}, \mathbf{s}) = \frac{1}{Z} e^{\sum_i b_i s_i + \sum_j c_j x_j + \sum_{i,j} s_i w_{i,j} x_j} \quad (26)$$

where Z is the partition function, which depends on the parameters \mathbf{b}, \mathbf{c} and \hat{w} that are learned from the data, in such a way as to maximise the log-likelihood $p(\mathbf{x})$. The energy of hidden state \mathbf{s} is defined as

$$E_{\mathbf{s}} = -\log p(\mathbf{s}) = \log Z - \sum_i b_i s_i - \sum_j \log \left[1 + e^{c_j + \sum_i s_i w_{i,j}} \right]. \quad (27)$$

We define the relevance with respect to a precision Δ of the energy spectrum. In order to do this, we define the probability

$$p_{\Delta}(E) = \sum_{\mathbf{s}: |E_{\mathbf{s}} - E| \leq \Delta/2} e^{-E_{\mathbf{s}}} \quad (28)$$

that a state \mathbf{s} has energy in the interval of width Δ around E . The relevance at precision Δ is defined as

$$H_{\Delta}[E] = - \sum_E p_{\Delta}(E) \log p_{\Delta}(E) \quad (29)$$

where the sum on E is restricted to integer multiples of Δ .

In what follows, we study a reduced MNIST dataset [16], where we first coarse grain the original 28×28 pixels data in cells of 2×2 pixels, that are transformed into binary values by applying a threshold¹². Finally we discard the first and the last rows and column of cells, thereby leaving us with a dataset of $N = 60000$ images of 12×12 binary pixels, corresponding to $n_v = 144$. The reason for working with such a reduced dataset is that it allows us to compute the exact distribution of energies, for values of n in a relevant range. Indeed, the evaluation of the energy requires the calculation of the partition function Z , which can be computed only for small systems. Sect. 4.1 presents results for RBMs with a number of hidden units such that the exact calculation of $p_\Delta(E)$ on all 2^n of states is within reach of our computational resources. For larger systems we sample $N \ll 2^n$ states \mathbf{s} from $p(\mathbf{s})$ with MCMC method and estimate $H_\Delta(E)$ from the sample (see Sect. 4.2).

As a reference, we take an ideal learning machine such that $H_\Delta[E]$ is maximal, at a fixed $H[\mathbf{s}]$. The ways in which this is computed parallels Ref. [13] and is detailed in Appendix B. As discussed in [13], the distinguishing feature of an ideal learning machine is that the degeneracy $W(E)$ of energy levels follows an exponential behaviour $W(E) \simeq W_0 e^{\nu E}$. In the present context, we define $W(E)$ as the number of energy levels in an interval of width Δ around E . We remark that the ideal limit confirms the scaling of entropic quantities with the number n of hidden variables found in the previous Section, i.e. $H[\mathbf{s}] \propto n$ and $H_\Delta[E] \propto \log n$.

We conclude this section by contrasting the analysis of RBMs with that of a Gaussian learning machine. This clarifies the meaning of the relevance in a learning task and its relation to feature extraction. Learning in the Gaussian case has nothing to do with the extraction of hidden features, because the features of the data that are relevant to learning are known *a priori* (e.g. mean and covariances). In loose words, there are no hidden features in a Gaussian world. Consistently, we shall see that the relevance stays constant during learning.

4.1 Exact energy spectrum for small systems

RBM's with $n \leq 24$ have been trained with ($K = 10$) contrastive divergence [23] on the data. We used mini-batches of 10^3 samples for the results shown in Fig. 8. Although these are not ideal for learning¹³, they allow us to monitor the dynamics of the RBM during learning, in the plane spanned by $H_\Delta[E]$ and $H[\mathbf{s}]$. As a function of Δ , the resolution is expected to behave as $H_\Delta[E] = h[E] - \log \Delta$, where $h[E]$ is the differential entropy [18] of the underlying probability density function of energy levels. Indeed we find that $H_\Delta[E] + \log \Delta$ is nearly constant in the range $0.1 < \Delta < 1$.

The sample digits generated from trained machines with $n = 10, 12, \dots, 24$, shown in the inset of Fig. 8 (left) appear rather noisy, as compared with digits generated with an RBM with $n = 50$ hidden units (see next section) and with a sample of ten original digits (top row). Our understanding is that the landscape of RBMs' likelihood function is characterised by several local maxima and our dynamics converges to one of them. At different point in time, we compute the full spectrum of energy levels and compute $H_\Delta[E]$ and $H[\mathbf{s}]$. Fig. 8 (left) suggests that learning occurs in cycles: A compression phase where $H[\mathbf{s}]$ decreases, followed by an expansion phase where the system comes closer to the ideal limit of a machine with maximal $H_\Delta[E]$ (dashed line).

Fig. 9 shows the evolution of the spectrum of energy levels which generates this dynamics. As

¹²If the sum of the grey levels of the four pixels exceeds 400, the coarse grained pixel is assigned the value one, otherwise it is zero.

¹³We confirmed that, as argued in [23], best performance is obtained with mini-batches of ~ 10 samples.

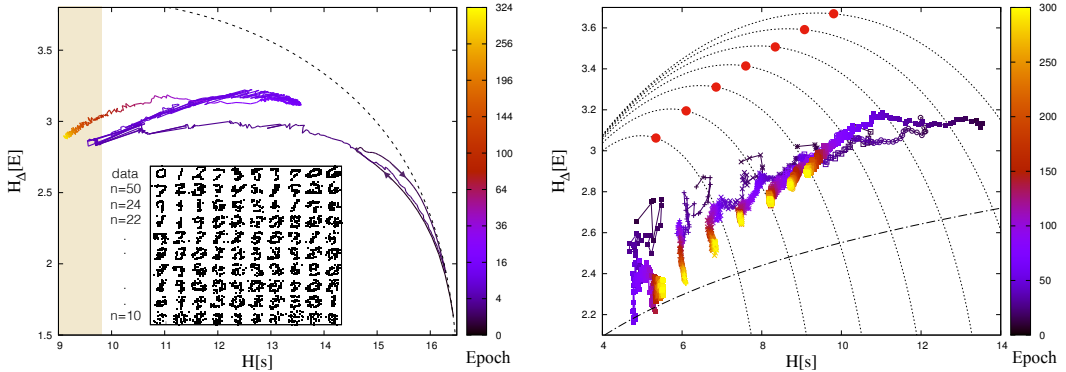


Figure 8: Left: typical trajectory during learning in the plane $(H[\mathbf{s}], H_{\Delta}[E])$ for a RBM with $n = 24$ trained on the reduced MNIST data ($\Delta = 0.5$). The ideal limit of maximal $H_{\Delta}[E] = h[E] - \log \Delta$ (see Appendix B) is shown as a dashed line. Inset: sample digits from the data (top row) and from trained RBM's with $n = 50, 24, 22, \dots, 12$ and 10, from top to bottom. Right: Late dynamics of training for RBM's with $n = 12, 14, \dots, 22$ and 24, from bottom left to top right. Dashed lines correspond to the ideal limit for different values of n . The red point marks the point where $h[E]$ is maximal. As a reference, the dot-dashed line shows the growth of $h[E]$ with n for a gaussian distribution with a variance proportional to n .

the bottom panel shows, the spectrum of energy levels expands more and more during training. At times ($n_e = 1, n_e = 10$) when the system is closer to the ideal limit (dashed line in Fig. 8), the degeneracy of energy levels develops a characteristic exponential behaviour $W(E) \simeq W_0 e^{\nu E}$, whereas it departs from it in the successive compression phases. In the late stages of the dynamics, for a given input \mathbf{x} , the distribution of internal states \mathbf{s} is sharply peaked. This makes it possible to map the dataset into a set of (clamped) internal states of the machine, as done in [14], and to compute the corresponding distribution $N(E)$ of energies. As shown in the top right panel of Fig. 9, the evolution of this distribution during learning follows the one of $p(E)$ and converges to a similar shape.

4.2 Measuring relevance with sampled internal states

When the number n of hidden variables is too large, it is not possible to compute exactly the spectrum of energy levels. On the other hand, the 2^n energy levels are learned from a sample of $N \ll 2^n$ data points, and we don't expect all details of the distribution of energies to be important. For this reason, we shall estimate $H_{\Delta}[E]$ to a precision of $\Delta = 1/N$, on the basis of a sample $\hat{\mathbf{s}} = (\mathbf{s}_1, \dots, \mathbf{s}_N)$ of N observations of the state \mathbf{s} of the hidden layer, drawn from the equilibrium distribution $p(\mathbf{s})$.

With a change of variables $f = e^{-E}$, we observe that

$$h[E] = - \int_0^1 df p(f) \log \left[p(f) \left| \frac{df}{dE} \right| \right] = h[f] + \langle E \rangle \quad (30)$$

Likewise, using $E_{\mathbf{s}} = -\log f_{\mathbf{s}}$,

$$H_{\Delta}[E] = H_{\Delta}[f] - \langle \log f \rangle \quad (31)$$

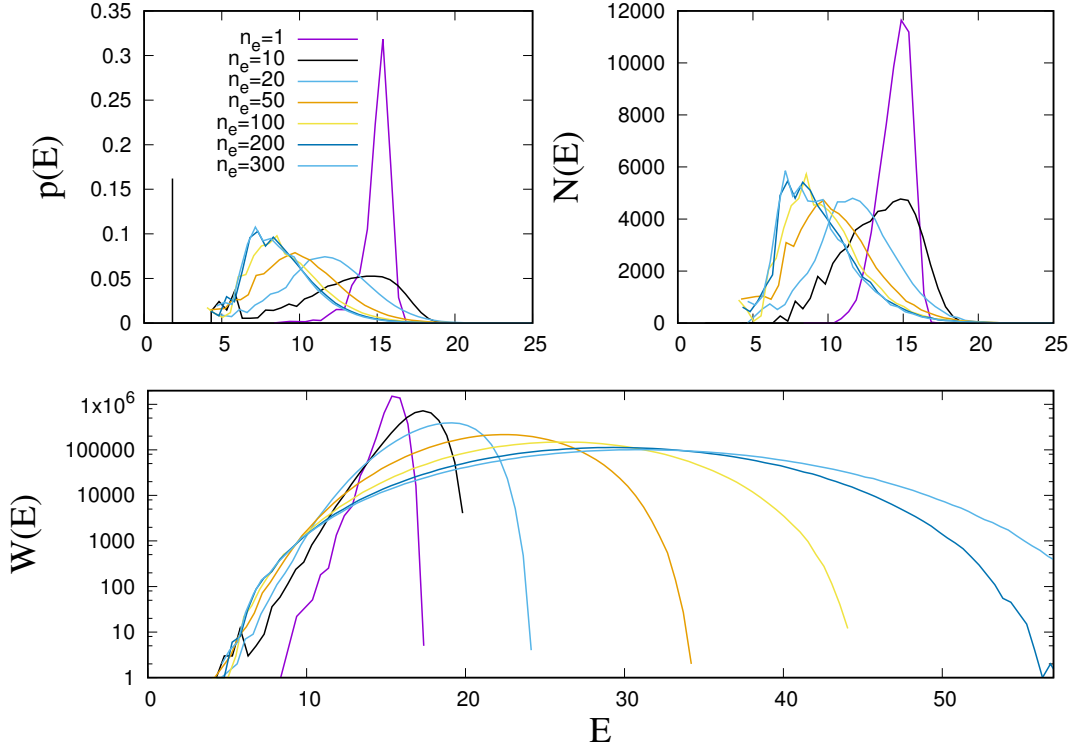


Figure 9: Distribution of energies ($p(E)$ - top left) and degeneracy of energy levels ($W(E)$ - bottom panel) for an RBM with $n = 22$ hidden units, during learning. The top right panel shows the corresponding distribution of the energies corresponding to the data points, i.e. the number $N(E)$ of data points that map to internal states of the machine with energy $E_s \in [E - \Delta/2, E + \Delta/2]$.

From the sample \hat{s} , we can compute the empirical distribution $\hat{f}_s = k_s/N$, where k_s is the number of times that state s occurs in the sample. The values of f_s are known to a precision $\Delta = 1/N$, and the probability distribution of f_s can be estimated from the sample observing that $P\{f_s = k/N\} = km_k/N$, where m_k is the number of states s that occur $k_s = k$ times in the sample. Hence $H_\Delta[f]$ can be computed as

$$H_\Delta[f] \simeq - \sum_k \frac{km_k}{N} \log \frac{km_k}{N} \equiv \hat{H}[k], \quad \Delta = \frac{1}{N}. \quad (32)$$

Likewise, the second term in Eq.(31) can be computed as

$$-\langle \log f \rangle \simeq - \sum_s \frac{k_s}{N} \log \frac{k_s}{N} \equiv \hat{H}[s]. \quad (33)$$

The two quantities $\hat{H}[s]$ and $\hat{H}[k]$ have been introduced earlier as a measure of resolution and relevance, respectively, within a sample [24, 25, 13].

Taken together, Eqs. (31, 32) and (33), imply

$$H_\Delta[E] \simeq \hat{H}[k] + \hat{H}[\mathbf{s}], \quad \Delta = \frac{1}{N}. \quad (34)$$

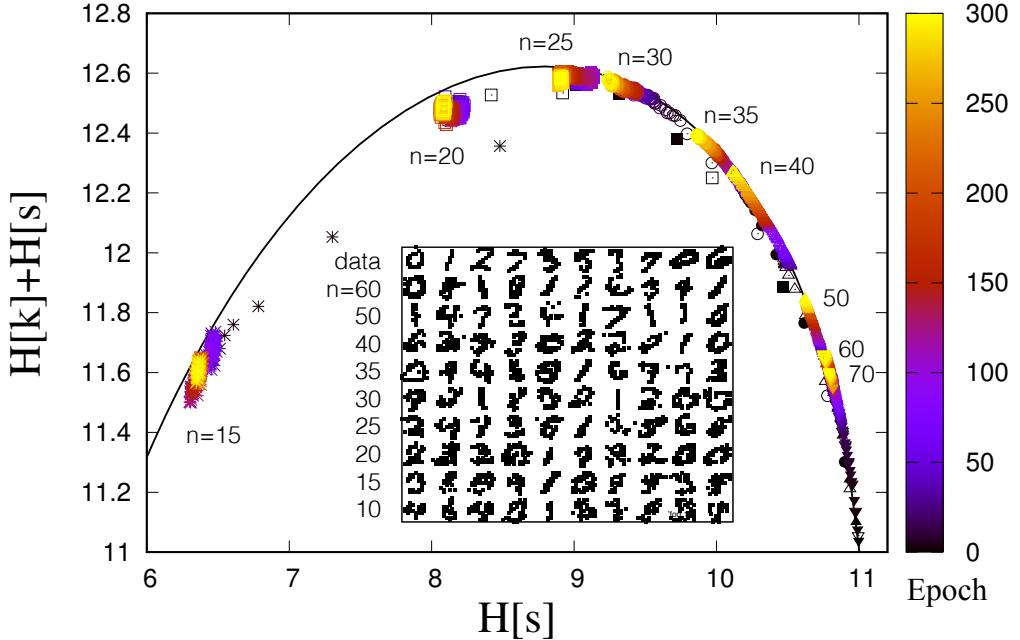


Figure 10: Relevance $H_\Delta[E] \simeq \hat{H}[k] + \hat{H}[\mathbf{s}]$ as a function of $\hat{H}[\mathbf{s}] \simeq \langle E \rangle$, for different training sessions of RBMs' with $n = 15, 20, 25, 30, 35, 40, 50, 60$ and 70 hidden nodes (from left to right). Each session was runs using persistent contrastive divergence [26] for 300 epochs with mini batches of 10 samples. The inset compares sample digits in the data (top row) with those drawn from $p(\mathbf{s})$ at the end of training for different n .

Fig. 10 reports the results of numerical experiments on the reduced MNIST dataset, with RBMs' with a number of hidden variables ranging from $n = 15$ to $n = 70$. Each training session lasts 300 epochs with persistent contrastive divergence [26]. The inset of Fig. 10 compares sample digits generated by the RBMs' with the original digits.

As a reference, we take the curve of maximal $\hat{H}[k]$ for a given $\hat{H}[\mathbf{s}]$ computed in [25]. This is shown as a full black line in Fig. 10. For each value of n , we observe trajectories in the $(H_\Delta[E], H[\mathbf{s}])$ plane that converge to points that are close to the theoretical curve where $\hat{H}[k] + \hat{H}[\mathbf{s}]$ is maximal, as first observed in [14].

In all cases we observe that the conditional entropy $H[\mathbf{s}|\mathbf{x}]$ decreases, implying that \mathbf{s} approaches a deterministic function of \mathbf{x} .

4.3 The Gaussian learning machine

Consider a Gaussian learning machine with m visible units $\mathbf{x} = (x_1, \dots, x_m)$ and n hidden units $\mathbf{s} = (s_1, \dots, s_n)$ which are all continuous variables. The joint probability distribution is given by

$$p(\mathbf{x}, \mathbf{s}) = \frac{1}{Z(\mathbf{b}, \hat{w})} e^{-\frac{1}{2}(\mathbf{x}-\mathbf{b})^2 - \frac{1}{2}\mathbf{s}^2 + \mathbf{x}'\hat{w}\mathbf{s}} \quad (35)$$

where prime denote transpose, $\mathbf{b} = (b_1, \dots, b_m)$ is a vector of parameters, \hat{w} is an $n \times m$ matrix of couplings, and $Z(\mathbf{b}, \hat{w})$ is a normalisation constant. The couplings \mathbf{b} and \hat{w} are adjusted so as to reproduce some data source

$$p(\mathbf{x}) = \frac{(2\pi)^{n/2}}{Z(\hat{w})} e^{-\frac{1}{2}(\mathbf{x}-\mathbf{b})^2 + \frac{1}{2}\mathbf{x}'\hat{w}\hat{w}'\mathbf{x}} \approx p_{\text{data}}(\mathbf{x}). \quad (36)$$

This machine learns the first two moments of the distribution of \mathbf{x} and it can be shown that it reconstructs the spectral components of an empirical covariance matrix with eigenvalue larger than one.

The distribution in the internal layer is¹⁴

$$p(\mathbf{s}) = \frac{(2\pi)^{m/2}}{Z(\mathbf{b}, \hat{w})} e^{-\frac{1}{2}\mathbf{s}'(1 - \hat{w}'\hat{w})\mathbf{s} + \mathbf{b}'\hat{w}\mathbf{s}} \quad (37)$$

so the energy is

$$E(\mathbf{s}) = \frac{1}{2}\mathbf{s}'(1 - \hat{w}'\hat{w})\mathbf{s} - \mathbf{b}'\hat{w}\mathbf{s} + \frac{m}{2}\log(2\pi) + \log Z(\mathbf{b}, \hat{w}) \quad (38)$$

$$= E_0(\hat{w}) + \frac{1}{2}(\mathbf{s} - \mathbf{s}_0)'(1 - \hat{w}'\hat{w})(\mathbf{s} - \mathbf{s}_0) \quad (39)$$

where

$$E_0(\hat{w}) = \frac{n}{2}\log(2\pi) - \log \sqrt{\det(1 - \hat{w}'\hat{w})} \quad (40)$$

is a constant (the ground state energy) and $\mathbf{s}_0(\mathbf{b}, \hat{w}) = (1 - \hat{w}'\hat{w})^{-1}\hat{w}\mathbf{b}$ is a vector. Notice that the resolution is given by:

$$H[\mathbf{s}] = \langle E \rangle = E_0(\hat{w}) + \frac{n}{2}. \quad (41)$$

The distribution of energies is

$$p(E) = \frac{1}{\Gamma(n/2)} (E - E_0)^{n/2-1} e^{-(E-E_0)}. \quad (42)$$

Remarkably, $p(E)$ is independent of \mathbf{b} and it depends on \hat{w} , i.e. on the data, only through the constant E_0 . Hence the differential entropy [18] of this distribution

$$h(E) = \frac{n}{2} + \log\left(\frac{n}{2}\right) - \left(\frac{n}{2} - 1\right) \log \psi\left(\frac{n}{2}\right) \simeq \frac{1}{2} \log(4\pi en) + O(1/n) \quad (43)$$

is independent of the parameters \mathbf{b}, \hat{w} . The scaling $h(E) \simeq \frac{1}{2}\log n$ for large n is consistent with the fact that asymptotically the distribution of energies is a Gaussian with variance proportional to n .

¹⁴The largest singular value of \hat{w} can be shown to be less than one, so that this is well defined.

Notice that \mathbf{s} is not a deterministic function of \mathbf{x} , because

$$p(\mathbf{s}|\mathbf{x}) = \frac{1}{(2\pi)^{n/2}} e^{-\frac{1}{2}(\mathbf{s}-\hat{w}\mathbf{x})^2}. \quad (44)$$

The conditional entropy of \mathbf{s} is given by $H[\mathbf{s}|\mathbf{x}] = \frac{n}{2} \log(2\pi e)$. Therefore, the amount of information learned from the data is given by (see Eqs. 40 and 41)

$$I(\mathbf{x}, \mathbf{s}) = H[\mathbf{s}] - H[\mathbf{s}|\mathbf{x}] = \frac{1}{2} \log \det \frac{1}{1 - \hat{w}'\hat{w}}. \quad (45)$$

Let us now comment these results in terms of the discussion in Section 2. There learning is discussed in terms of the extraction of hidden features (the sufficient statistics) from the data, and $H[E]$ provides a lower bound to the amount of information that is learned. In the Gaussian learning machine, the sufficient statistics are known from the outset, i.e. $\phi(\mathbf{s}) = \{s_i, s_i s_j, i \leq j = 1, \dots, n\}$, so learning is only about the parameters. There is no learning on hidden features, because the generative model remains a Gaussian distribution, whatever the data is. This is why $h[E]$ is independent of the data. Rather, learning occurs via an increase of the resolution $H[\mathbf{s}]$, that measures the information gained on the data, through the parameters.

The inequality (9) $I(\mathbf{s}, \phi) \geq H[E]$ is always true. Yet this does not allow us to draw conclusions on $I(\mathbf{x}, \phi)$ because \mathbf{s} is far from being a deterministic function of \mathbf{x} (see Eq. 44).

The findings in the section confirm that the Gaussian multivariate model has a special place in statistical inference (see e.g. [27]) and the generalisation of conclusions drawn from it should be taken with care.

5 Conclusion

Maximal relevance has been proposed as a principle that characterises optimal learning machines [13]. A distinctive feature of an approach based on maximal relevance is that it allows us to discuss the properties of OLMs without any reference to the data they have been trained with, as long as this is sufficiently structured. For example, Ref. [28] has shown that systems with an exponential distribution of energy levels, that correspond those that achieve maximal relevance, exhibit rather peculiar statistical mechanics properties.

The first contribution of this paper is to provide a clear relation between the relevance and hidden features in learning. We show that the relevance $H[E]$ provides a lower bound to the mutual information between the state of the machine and the hidden features that a learning machine is supposed to extract (see Section 2). The principle of maximal relevance then pushes the architecture of the learning machine to detect maximally informative features. This result is a characterisation of typical learning machines. It does not exclude the existence of efficient learning machines with low values of $H[E]$. Rather it insures that learning machine with high values of $H[E]$ provide at least that much information on the hidden features.

The second contribution of this paper is to investigate architectures that achieve maximal relevance, and to test whether the internal representations of well trained learning machines approach this limit or not. We first study optimal learning machines in the context of a well defined class of models – the fully connected Ising models with binary couplings. Compared to architectures actually used in deep learning, this is manifestly a toy model. Yet it sheds light on the properties responsible for the spectacular performance of learning machines, contributing to the literature on

the statistical mechanics of learning [4, 6, 7, 5]. We show that these properties may be related to sub-extensive quantities in the statistical mechanics treatment. This suggests that learning machines are characterised by properties that may not be accessible to a treatment that focuses only on leading thermodynamic terms. A proper understanding of these systems requires a detailed analysis of fluctuations around the saddle point. This result also tallies with observation that complexity reveals itself in the sub-extensive contribution to the entropy, both in statistical models¹⁵ [29, 19] and in time series¹⁶ [30]. We find that Ising OLMs feature a majority of ferromagnetic interactions. This implies that their ground state is ferromagnetic (in the fixed gauge adopted here), with a wide distribution of energy levels as observed in [13]. Each OLM is realised by a set of interaction matrices \mathcal{J} with a large degeneracy. Local update rule that imply the rewiring of a single negative coupling can explore a large part of this set, suggesting that the relevance $H[\mathcal{E}]$ is characterised by wide flat maxima in the space of the parameters $\hat{\mathcal{J}}$. It is tempting to relate this property to that discussed by [6].

These results also contribute to the discussion on the criticality of learned models [31, 7, 32]. We confirm that models such as the MFIFM or the star model, have a superior learning performance when poised at the critical point. Yet, it is not strictly necessary for an OLM to be poised at a critical point marking the transition between two different phases. Indeed, we find recursive models with a learning performance superior to that of models that feature a phase transition, in a wide range of the resolution scale.

Next we generalise the analysis to learning machines with continuous energy levels. We analyse learning dynamics of RBMs on a reduced MNIST dataset and show that RBMs expand their energy spectrum during learning, to a remarkable extent. This suggests that learning occurs in cycles of compression – with a decreases in resolution – and expansion – with an increase in relevance. The trajectory stays below the ideal limit of maximal relevance, which we believe reflects the fact that the size of the training set limits the amount of information that the machine can extract from the data. Indeed, when resolution and relevance are measured with respect to a sample of the same size of the training set, we find that RBMs approach the curve of maximal relevance attainable at a given resolution.

Finally we discuss learning in a Gaussian machine that aims at reproducing means and covariances of a dataset. We show that in this case the relevance is independent of the data and that information gain is only accounted for by a change in resolution. We argue that this is consistent with the fact that the features that the machine learns are predefined by the structure of the model, in this case. There is no learning on the generative model, that remains a multivariate normal distribution. This example clarifies the meaning the relevance and the difference between learning and parameter inference.

We hope that these results will not only contribute to our understanding of learning machines, but that they may also pave the way to applications that may improve further the performance of learning machines.

¹⁵Minimum Description Length, as well as Bayesian inference, identify the leading order term that should be used in model selection to penalise the likelihood of models for their complexity. In both cases this term is $\frac{d}{2} \log N$, where d is the number of parameters of the model and N is the number of data points. This term is sub-leading with respect to the log-likelihood, which is proportional to N .

¹⁶The complexity of a time series is defined in [30] as the predictive information, which is the mutual information between the recent past, in a window of T time points, and the future of the time series.

Acknowledgments

We're benefitted from discussions with Jean Barbier, Riccardo Zecchina, Federico Ricci-Tersenghi and Yasser Roudi. We are grateful to the authors of Re. [22] for sharing their data with us. We thank an anonymous referee of MSML2020 for pointing out the example in Section 4.3.

References

- [1] J. J. Hopfield, “Neural networks and physical systems with emergent collective computational abilities,” *Proc Natl Acad Sci U S A*, vol. 79, no. 8, pp. 2554–8, 1982.
- [2] D. H. Ackley, G. E. Hinton, and T. J. Sejnowski, “A learning algorithm for boltzmann machines*,” *Cognitive Science*, vol. 9, no. 1, pp. 147–169, 1985.
- [3] M. Baity-Jesi, L. Sagun, M. Geiger, S. Spigler, G. B. Arous, C. Cammarota, Y. LeCun, M. Wyart, and G. Biroli, “Comparing dynamics: Deep neural networks versus glassy systems,” in *Proceedings of the 35th International Conference on Machine Learning* (J. Dy and A. Krause, eds.), vol. 80 of *Proceedings of Machine Learning Research*, (Stockholmsmässan, Stockholm Sweden), pp. 314–323, PMLR, 10–15 Jul 2018.
- [4] J. Tubiana and R. Monasson, “Emergence of compositional representations in restricted boltzmann machines,” *Physical review letters*, vol. 118, no. 13, p. 138301, 2017.
- [5] A. Decelle, G. Fissore, and C. Furtlehner, “Thermodynamics of restricted boltzmann machines and related learning dynamics,” *Journal of Statistical Physics*, vol. 172, pp. 1576–1608, Sep 2018.
- [6] C. Baldassi, C. Borgs, J. T. Chayes, A. Ingrosso, C. Lucibello, L. Sagietti, and R. Zecchina, “Unreasonable effectiveness of learning neural networks: From accessible states and robust ensembles to basic algorithmic schemes,” *Proceedings of the National Academy of Sciences*, vol. 113, no. 48, pp. E7655–E7662, 2016.
- [7] M. E. Rule, M. Sorbaro, and M. H. Hennig, “Optimal encoding in stochastic latent-variable Models,” *ArXiv e-prints*, p. arXiv:1802.10361, Feb. 2018.
- [8] M. Mézard, “Mean-field message-passing equations in the hopfield model and its generalizations,” *Phys. Rev. E*, vol. 95, p. 022117, Feb 2017.
- [9] S. Goldt, M. Mézard, F. Krzakala, and L. Zdeborová, “Modelling the influence of data structure on learning in neural networks,” *arXiv preprint arXiv:1909.11500*, 2019.
- [10] P. Rotondo, M. C. Lagomarsino, and M. Gherardi, “Counting the learnable functions of geometrically structured data,” *Phys. Rev. Research*, vol. 2, p. 023169, May 2020.
- [11] L. Zdeborová, “Understanding deep learning is also a job for physicists,” *Nature Physics*, pp. 1–3, 2020.
- [12] S. Carnot, “Réflexions sur la puissance motrice du feu et sur les machines propres à développer cette puissance,” in *Annales scientifiques de l’École Normale Supérieure*, vol. 1, pp. 393–457, 1872.

- [13] R. J. Cubero, J. Jo, M. Marsili, Y. Roudi, and J. Song, “Statistical criticality arises in most informative representations,” *Journal of Statistical Mechanics: Theory and Experiment*, vol. 2019, p. 063402, jun 2019.
- [14] J. Song, M. Marsili, and J. Jo, “Resolution and relevance trade-offs in deep learning,” *Journal of Statistical Mechanics: Theory and Experiment*, vol. 2018, p. 123406, dec 2018.
- [15] R. Cubero, M. Marsili, and Y. Roudi, “Minimum description length codes are critical,” *Entropy*, vol. 20, p. 755, Oct 2018.
- [16] Y. LeCun, L. Bottou, Y. Bengio, and P. Haffner, “Gradient-based learning applied to document recognition,” *Proceedings of the IEEE*, vol. 86, no. 11, pp. 2278–2324, 1998.
- [17] D. J. Schwab, I. Nemenman, and P. Mehta, “Zipf’s law and criticality in multivariate data without fine-tuning,” *Phys. Rev. Lett.*, vol. 113, p. 068102, Aug 2014.
- [18] T. M. Cover and J. A. Thomas, *Elements of information theory*. John Wiley & Sons, 2012.
- [19] I. J. Myung, V. Balasubramanian, and M. A. Pitt, “Counting probability distributions: Differential geometry and model selection,” *Proceedings of the National Academy of Sciences*, vol. 97, no. 21, pp. 11170–11175, 2000.
- [20] R. J. Cubero, M. Marsili, and Y. Roudi, “Finding informative neurons in the brain using Multi-Scale Relevance,” *ArXiv e-prints*, Feb. 2018.
- [21] S. Jonhson, V. Dominguez-Garcia, and M. A. Muñoz, “Factors determining nestedness in complex networks,” *PLoS One*, vol. 8, no. 9, p. e74025, 2013.
- [22] E. D. Lee, C. P. Broedersz, and W. Bialek, “Statistical Mechanics of the US Supreme Court,” *Journal of Statistical Physics*, vol. 160, pp. 275–301, July 2015.
- [23] G. E. Hinton, “A practical guide to training restricted boltzmann machines,” in *Neural networks: Tricks of the trade*, pp. 599–619, Springer, 2012.
- [24] M. Marsili, I. Mastromatteo, and Y. Roudi, “On sampling and modeling complex systems,” *Journal of Statistical Mechanics: Theory and Experiment*, vol. 2013, no. 09, p. P09003, 2013.
- [25] A. Haimovici and M. Marsili, “Criticality of mostly informative samples: a bayesian model selection approach,” *Journal of Statistical Mechanics: Theory and Experiment*, vol. 2015, no. 10, p. P10013, 2015.
- [26] T. Tieleman, “Training restricted boltzmann machines using approximations to the likelihood gradient,” in *Proceedings of the 25th international conference on Machine learning*, pp. 1064–1071, 2008.
- [27] M. Tumminello, F. Lillo, and R. N. Mantegna, “Kullback-leibler distance as a measure of the information filtered from multivariate data,” *Phys. Rev. E*, vol. 76, p. 031123, Sep 2007.
- [28] M. Marsili, “The peculiar statistical mechanics of Optimal Learning Machines,” *ArXiv e-prints*, p. arXiv:1904.09144, Feb. 2018.

- [29] G. Schwarz, “Estimating the dimension of a model,” *Ann. Statist.*, vol. 6, pp. 461–464, 03 1978.
- [30] W. Bialek, I. Nemenman, and N. Tishby, “Predictability, complexity, and learning,” *Neural Computation*, vol. 13, no. 11, pp. 2409–2463, 2001.
- [31] I. Mastromatteo and M. Marsili, “On the criticality of inferred models,” *Journal of Statistical Mechanics: Theory and Experiment*, vol. 2011, no. 10, p. P10012, 2011.
- [32] M. A. Muñoz, “Colloquium: Criticality and dynamical scaling in living systems,” *Rev. Mod. Phys.*, vol. 90, p. 031001, Jul 2018.

A Asymptotic value of h_E for the MFIFM

The distribution of energy levels is given by $p(E) = W(E)e^{-E}/Z$, where $Z = \sum_E W(E)e^{-E}$. Hence the relevance is given by

$$H[E] = \log Z - \langle \log W(E) \rangle + \langle E \rangle. \quad (46)$$

The degeneracy of energy level E_m in Eq. (19) is

$$W(E_m) = 2 \binom{n}{\frac{n+m}{2}} \simeq \sqrt{\frac{2}{\pi n(1-\mu^2)}} e^{nS(\mu)}, \quad \mu = \frac{m}{n} \in [-1, 1]$$

where $S(\mu) = -\frac{1+\mu}{2} \log \frac{1+\mu}{2} - \frac{1-\mu}{2} \log \frac{1-\mu}{2}$. In the regime where $h_s \in [0, 1]$ is finite, J is of order $1/n$ and, for $n \rightarrow \infty$, the partition function is dominated by the saddle point $\mu^* = \arg \min_\mu f(\mu)$ with $f(\mu) = Jn\mu^2/2 - S(\mu)$. For $Jn \neq 1$, the first term in Eq. (46) can be computed with integration over the gaussian fluctuations

$$Z \simeq \sqrt{\frac{2n}{\pi}} \int_{-1}^1 \frac{d\mu}{\sqrt{1-\mu^2}} e^{-nf(\mu)} \simeq \sqrt{\frac{2}{\pi(1-\mu^{*2})f''(\mu^*)}} e^{-nf(\mu^*)}$$

Here, the \sqrt{n} factor is canceled because $f(\mu) - f(\mu^*) \sim (\mu - \mu^*)^2$, and the change of variables $z = \sqrt{n}(\mu - \mu^*)$ generates a $1/\sqrt{n}$ term.

Hence $\log Z \simeq -nf(\mu^*) + \text{const}$. The extensive term in $\log Z$ is canceled by an analogous term in

$$\langle \log W(E) \rangle - \langle E \rangle \simeq nf(\mu^*) + \log \sqrt{2\pi n(1-\mu^2)}$$

so, to leading order, $H[E] \simeq \frac{1}{2} \log n + \text{const}$, which implies $h_E \rightarrow 1/2$ as $n \rightarrow \infty$.

For $Jn = 1$, instead, $f(\mu) - f(\mu^*) \simeq a(\mu - \mu^*)^4 + \dots$. This implies that in the calculation of Z we need a change of variables $z = n^{1/4}(\mu - \mu^*)$ that yields $\log Z \simeq \frac{1}{4} \log n + \text{const}$. This additional term is responsible for the asymptotic behaviour $h_E \rightarrow 3/4$ for $Jn = 1$.

B An ideal limit of an Optimal Learning Machine

In the case $n \gg 1$ of a learning machine with many hidden units, we can approximate the distribution of energies with a continuous probability density $p(E)$, that we assumed to be defined in an interval $E \in [0, \bar{E}]$. For Δ small enough, the behaviour of $H_\Delta[E]$ with Δ is given by

$$H_\Delta[E] \simeq h[E] - \log \Delta \quad (47)$$

where $h[E]$ is the differential entropy [18]

$$h[E] = - \int_0^{\bar{E}} dE p(E) \log p(E). \quad (48)$$

For a fixed Δ , the ideal limit of a learning machine with maximal $H_\Delta[E]$ is then obtained by finding the $p(E)$ that makes $h[E]$ maximal.

Let $W(E)$ be the density of energy levels, i.e. $W(E)dE$ is the number of states s with $E_s \in [E, E + dE]$. The probability density function $p(E)$ is then given by $p(E) = W(E)e^{-E}$. The Ideal Learning Machine is defined by the solution of the optimisation problem

$$W^*(E) = \arg \max_{W(E)} h[E] \quad (49)$$

$$\text{s.t. } H[\mathbf{s}] = \langle E \rangle \quad (50)$$

$$\int_0^{\bar{E}} W(E)dE = N \quad (51)$$

$$\int_0^{\bar{E}} W(E)e^{-E}dE = 1, \quad (52)$$

where

$$h[E] = - \int_0^{\bar{E}} dE p(E) \log p(E) = \langle E \rangle - \langle \log W(E) \rangle. \quad (53)$$

The solution of this problem is found introducing Lagrange multipliers to enforce the constraints (50,52), and fixing \bar{E} to satisfy Eq. (51). The solution reads

$$W(E) = \frac{\nu}{e^{\nu\bar{E}} - 1} e^{(1+\nu)\bar{E}}, \quad (54)$$

$$H[\mathbf{s}] = \langle E \rangle = \frac{\bar{E}}{1 - e^{-\nu\bar{E}}} - \frac{1}{\nu}, \quad (55)$$

$$h[E] = \log \frac{e^{\nu\bar{E}} - 1}{\nu} - \frac{\nu\bar{E}}{1 - e^{-\nu\bar{E}}} + 1, \quad (56)$$

$$N = \frac{\nu}{1 + \nu} \frac{e^{(1+\nu)\bar{E}} - 1}{e^{\nu\bar{E}} - 1}, \quad (57)$$

where Eq. (57) needs to be solved to obtain \bar{E} as a function of N and Eq. (55) yields ν as a function of $H[\mathbf{s}]$. The limit $\nu \rightarrow 0$ is revealing to understand the scaling of $H[\mathbf{s}]$ and $h[E]$ on N . We find

$$\bar{E} = \log(1 + N\bar{E}) \simeq \log N + \log \log N + O\left(\frac{\log \log N}{\log N}\right) \quad (\nu = 1) \quad (58)$$

$$H[\mathbf{s}] = \frac{1}{2}\bar{E} \simeq \frac{1}{2}\log N \quad (59)$$

$$h[E] = \log \bar{E} \simeq \log \log N. \quad (60)$$

At this point, the curve $h[E]$ vs $H[\mathbf{s}]$ is close to its maximum. So Eq. (60) provides an upper bound on the possible value of $h[E]$. In the case of a Boltzmann machine with n hidden units, there are $N = 2^n$ hidden states. Hence $H[\mathbf{s}]$ grows linearly with n and $H[E] \propto \log n$ grows with

the logarithm of the number of hidden units n . This is the same scaling that we have found for discrete energy levels.

When it is possible to compute the full spectrum of energy levels, we compare the results of learning experiments with those obtained in this ideal limit with $N = 2^n$. When instead $H[E]$ is estimated on a sample of N points, then the correct benchmark is given by the solution above with N being the size of the sample.